

# Open chemical reaction networks, steady-state loads and Braess-like paradox

Kinshuk Banerjee and Kamal Bhattacharyya<sup>1</sup>

*Department of Chemistry, University of Calcutta, 92 A.P.C. Road, Kolkata 700 009, India.*

## Abstract

Open chemical reaction systems involve matter-exchange with the surroundings. As a result, species can accumulate inside a system during the course of the reaction. We study the role of network topology in governing the concentration build-up inside a fixed reaction volume at steady state, particularly focusing on the effect of additional paths. The problem is akin to that in traffic networks where an extra route, surprisingly, can *increase* the overall travel time. This is known as the Braess' paradox. Here, we report chemical analogues of such a paradox in suitably chosen reaction networks, where extra reaction step(s) can *inflate* the total concentration, denoted as 'load', at steady state. It is shown that, such counter-intuitive behavior emerges in a qualitatively similar pattern in networks of varying complexities. We then explore how such extra routes affect the load in a biochemical scheme of uric acid degradation. From a thorough analysis of this network, we propose a functional role of some decomposition steps that can trim the load, indicating the importance of the latter in the evolution of reaction mechanisms in living matter.

Keywords: Open system; Steady flow; Network; Routing

## 1 Introduction

Open chemical systems remain an active field of research, particularly due to their link with a broad class of areas starting from living organisms to industrial processes [1, 2, 3, 4, 5, 6, 7]. Emergence of features like sustained oscillation [8] and multistability [9] in open chemical reaction networks (CRNs) [10] have intimate relations with physiological functions like circadian rhythms [11] and cellular differentiation [12]. Complex CRNs exchanging matter (and energy) with the environment are of prime importance in

---

<sup>1</sup>Corresponding author; e-mail: pchemkb@gmail.com

biology, *e.g.*, metabolic [13], neural [14], gene [15] and protein networks [16]. Comparatively small-scale CRNs are ubiquitous in the form of tautomeric equilibria, important in many biological processes, *e.g.*, in the chemical versatility of thiamin [17] and in spontaneous mutation [18].

Open systems involve flow of material, even in the steady state (SS), and necessarily describe out-of-equilibrium situations [19, 20, 21]. So, they continue to play a fundamental role in the development of non-equilibrium thermodynamics [22, 23, 24, 25] and, in turn, to understand the effects of such far-from-equilibrium scenarios on system functionality [26, 27, 28]. The major points of departure in the behavior of an open system compared to a closed system are the following: (i) Open systems can support a (non-equilibrium) SS whereas closed systems attain thermodynamic equilibrium [27]; (ii) The SS composition depends on the dynamics, *i.e.*, on the values of the dynamical parameters (rate constants and matter flows); but, in an equilibrium state, the concentrations are constrained by thermodynamics, *i.e.*, by equilibrium constants (ratios of rate constants). The wealth of behaviors emerging in such (non-equilibrium) SS have generated, over the years, a lot of attention regarding its role in biochemical environments residing far-from-equilibrium. Some notable applications are kinetic proofreading [29], energy transduction [30], optimization of reaction yield [31], information acquisition in DNA replication [32] etc.

The theoretical modeling of open CRNs is often based on the chemiostatic condition [33, 34, 35] that still holds a key place in the irreversible thermodynamic description of such networks [36]. As the name suggests, here concentrations of some of the reacting species are taken time-independent throughout the course of the reaction. In many instances, this leads to a simplification of the problem by converting certain non-linear kinetic equations to linear ones [27, 33, 35]. In this type of situation, however, the matter-exchange with the surroundings is *not* taken into account directly in the formulation of rate equations. Here, though, we treat the kinetics by explicitly including the matter-flow.

In an open CRN, the build-up of reacting species depends on the system parameters. The latter include the rates of inflow, outflow and the reaction constants. Here, we denote the total accumulated material inside the (fixed) reaction volume as the ‘load’. It is the sum of concentrations of all the species in the reaction medium. In a closed system, with mass-conservation being valid, the load remains the same throughout the course of the reaction. So, the concept of load is relevant only for open chemical systems where mass-

conservation is broken. However, it seems that such a quantity did not attract much attention. The magnitude of the load is important because a high value of a component may lead to undesirable side-reactions such as aggregation; the effects of activity coefficients get pronounced as well. Also, for a given SS flow, there must be an upper limit of the load which the reaction volume can sustain. Hence, it is important to understand the roles of the network structure and system parameters in governing the SS load. This knowledge can then be utilized to formulate strategies to reduce the load by properly modifying the network for an optimized flow [37]. This is also crucial in traffic networks where one can take the total number of vehicles in various terminuses or traffic signals as the load. However, the plan of adding new paths (roads) to trim the load and/or improve the flow does *not* succeed always. In the context of traffic flow, addition of a road of much better quality may lead to an *increase* in the overall travel time from a given source to destination for each traveller. This is known as the Braess' paradox (BP) [38, 39], after Dietrich Braess, who introduced this concept regarding traffic assignment problems. The BP also occurs in electrical, mechanical and thermal networks [40, 41]. For example, BP is manifested in the conductance drop of a branched semiconductor mesoscopic network when an extra branch is added [42]. A recent study also reports BP in a chemical system where an additional reaction step results in the lowering of product-formation rate [43].

In this work, we consider an open CRN, starting from a basic four-node structure as shown in Fig.1. The dashed (red) line BC in Fig.1 represents the extra path which can be uni- or bi-directional. Specific chemical examples of such networks are tautomeric (and conformational) equilibria of hydrazones derived from hydroxyl naphthaldehydes where the extra path is absent [44] and tautomeric equilibria of 6-(2-pyrrolyl)pyridazines where the extra path is present [45]. Keto-enol and imine-enamine tautomerism of 2-, 3- and 4-Phenacylpyridines [46] and imine-enamine tautomerism of the enzyme glyoxylate carboligase [47] also involve four-node networks or subnetworks with or without the extra path. Our goal here is to study the effect of the extra path on the load, *i.e.*, the total concentration of the reacting species, at SS. The presence of the extra path is expected to decrease the load as it opens up a new avenue of transport. Thus, a rise in the load when the extra path is operative can be designated as a BP-like behavior. In Sec.2, we first study a CRN similar to that shown in Fig.1 where, except the extra path, all the other steps are irreversible. In Sec.3, some of the steps are made reversible.

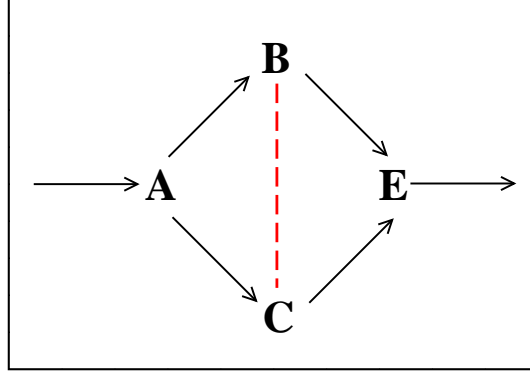


Figure 1: Schematic diagram of an open network. The presence of the extra path (dashed, red line), which can be uni- or bi-directional, is expected to reduce the load at steady state. However, this may not *always* be the case, leading to a Braess-like paradox.

The network is extended to a six-node one in Sec.4. In all the cases, we find that BP-like features appear with a qualitatively similar pattern. In Sec.5, the methodology is applied to a CRN of biological relevance. The overall outcomes are finally summarized in Sec.6.

## 2 A network with irreversible edges

A simple CRN is shown in Fig.2. We call this network Scheme I. Here,  $\gamma_0$  is the *constant* rate of injection of species A into the reaction system of fixed volume and  $k_i$  are the (first-order) rate constants. Species E goes out of the system via a process having rate constant  $k_6$ . The time-dependent concentrations of species A, B, C, E are denoted by  $a(t), b(t), c(t), e(t)$ , respectively. Thus, the load  $Z(t)$  of this system is

$$Z(t) = a(t) + b(t) + c(t) + e(t). \quad (1)$$

The thermodynamic fluxes[20]  $J_i$  ( $i = 0, 1, \dots, 6$ ) are given by

$$J_0 = \gamma_0, J_1(t) = k_1 a(t), J_2(t) = k_2 b(t), J_3(t) = k_3 a(t),$$

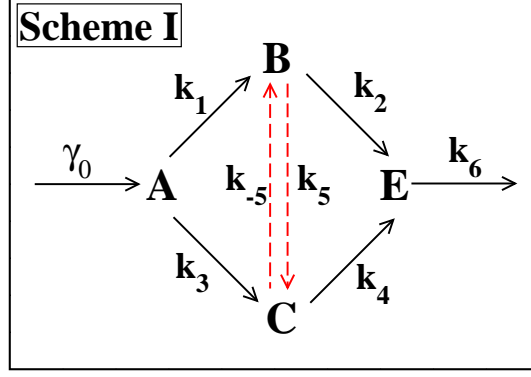


Figure 2: Schematic diagram of a CRN with irreversible edges. The extra path is shown by the dashed, red line.

$$J_4(t) = k_4 b(t), J_5(t) = k_5 b(t) - k_{-5} c(t), J_6(t) = k_6 e(t). \quad (2)$$

The reason for introducing these fluxes will become clear later. Now, the kinetic equations can be expressed in terms of  $J_i$  as follows

$$\dot{a}(t) = J_0 - J_1(t) - J_3(t) \quad (3)$$

$$\dot{b}(t) = J_1(t) - J_2(t) - J_5(t) \quad (4)$$

$$\dot{c}(t) = J_3(t) + J_5(t) - J_4(t) \quad (5)$$

$$\dot{e}(t) = J_2(t) + J_4(t) - J_6(t). \quad (6)$$

At steady state (SS), we have  $\dot{a} = \dot{b} = \dot{c} = \dot{e} = 0$  and hence,  $J_0 = J_6$  (the SS values are represented by omitting the time-argument). From Eqs.(2)-(6), one gets the SS concentrations as

$$a = \gamma_0 / (k_1 + k_3) \quad (7)$$

$$b = \frac{\gamma_0(k_4 + k_{-5}) - ak_3k_4}{k_2(k_4 + k_{-5}) + k_4k_5} \quad (8)$$

$$c = \frac{\gamma_0k_5 + ak_2k_3}{k_2(k_4 + k_{-5}) + k_4k_5} \quad (9)$$

$$e = \gamma_0/k_6. \quad (10)$$

It is important to note that, the SS concentrations do *not* depend on the initial condition, *i.e.*, the set of concentrations at  $t = 0$ . In what follows, we mainly concentrate on the load  $Z$  defined in Eq.(1) at the SS.

## 2.1 Effect of extra path on the load

Our focus now is on the reaction path BC with rate constants  $k_{\pm 5}$  that acts as the extra path. It is expected that, presence of this extra path should enhance the transport efficiency and hence decrease the load  $Z$  of the system at SS. To measure the effect of extra path on  $Z$ , we introduce the load-difference  $\Delta$  defined as

$$\Delta = Z^0 - Z \quad (11)$$

where  $Z^0$  is the value of  $Z$  when  $k_{\pm 5} = 0$ . For finite non-zero values of  $k_5$  and/or  $k_{-5}$ ,  $\Delta$  is expected to be positive. We will investigate whether this is *always* the case. If, for a set of parameter values,  $\Delta$  comes out to be negative (or zero), then it is a counter-intuitive behavior analogous to the BP. We call any such region of parameter space with  $\Delta \leq 0$  as the BP zone. The SS concentrations at  $k_{\pm 5} = 0$  are similarly denoted by a zero superscript with  $a^0 = a$ ,  $e^0 = e$ .

Using Eqs.(8)-(9),  $J_5$ , the flux of the extra path, at the SS reads as

$$J_5 = \frac{\gamma_0(k_1 k_4 k_5 - k_2 k_3 k_{-5})}{(k_1 + k_3)(k_2(k_4 + k_{-5}) + k_4 k_5)}. \quad (12)$$

$J_5 > 0$  means the (net) flow in the extra path is in the direction  $B \rightarrow C$  and  $J_5 < 0$  indicates that the flow is reversed. Now, using Eqs.(7)-(12), we can relate  $\Delta$  with  $J_5$  by

$$\Delta = (b^0 + c^0) - (b + c) = \left( \frac{k_4 - k_2}{k_2 k_4} \right) J_5. \quad (13)$$

## 2.2 Emergence of BP zone: finite and infinite

From Eq.(12) and Eq.(13), one can see that  $\Delta$ , viewed as a function of  $k_4$ , becomes zero at

$$k_4 = \left( \frac{k_2 k_3 k_{-5}}{k_1 k_5} \right) \text{ and } k_4 = k_2. \quad (14)$$

$J_5$  is zero at the first solution in Eq.(14). So  $\Delta$  *changes sign twice* as a function of  $k_4$ . When  $k_4$  is much smaller than the other rate constants, it follows from Eqs.(12)-(13) that  $\Delta$  is large and positive. As  $k_4$  increases,  $\Delta$  decreases and becomes zero at the first or the second value of  $k_4$  given in Eq.(14), depending on whether  $k_3k_{-5} < k_1k_5$  or not. Between these two values,  $\Delta$  remains *negative*. Thus, the extra path leads to an *increase* in load over a *finite region* of parameter space. We call this region the *finite BP zone*. It is easy to check that  $\Delta$  shows a similar behavior as a function of  $k_2$ . However, as a function of any other rate constant,  $\Delta$  changes sign *only* once and, depending on the parameter values, it can remain negative for a large range, approaching zero asymptotically. This results in an *infinite BP zone*. According to Eq.(13),  $\Delta$  vanishes for  $k_4 = k_2$  and the system is *always* in the BP zone. This is interesting, as then one can *never* ‘gain’ by adding the extra path whatever be its (or other paths’) characteristics.

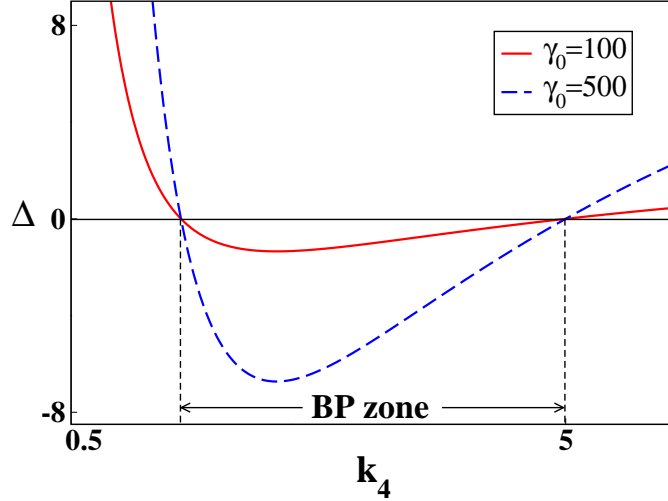


Figure 3: Variations of  $\Delta$  as a function of  $k_4$  for different  $\gamma_0$  for the network in Scheme I. The values of the parameters are as follows:  $k_1 = 1.0$ ,  $k_2 = 5.0$ ,  $k_3 = 1.5$ ,  $k_6 = 10.0$ ,  $k_5 = 5.0$ ,  $k_{-5} = 1.0$ , all in  $\text{s}^{-1}$  and  $\gamma_0$  is in  $\text{Ms}^{-1}$  unit.

## 2.3 Role of influx

It is important to note also from Eqs.(12)-(13) that, when other parameters are kept fixed,  $\Delta$  is proportional to  $\gamma_0$ . Thus, the gain in adding the extra path is higher for a larger  $\gamma_0$  in a non-BP zone ( $\Delta > 0$ ). But, so is the loss when the system resides in a BP zone. This feature is depicted in Fig.3 by plotting  $\Delta$  as a function  $k_4$  for two values of  $\gamma_0$  (in  $\text{Ms}^{-1}$ ). The BP zone is indicated explicitly in the figure, bounded by the two values of  $k_4$  given by Eq.(14). Thus, for a network in the BP zone, the increase in load (after inclusion of extra path) can be extremely hazardous if it reaches or surpasses the inherent capacity. One can see from Fig.3 that the variation of  $\Delta$  is much sharper at smaller values of  $k_4$ . So, the transition from non-BP zone to BP zone can occur by a very minor alteration of  $k_4$ , particularly at higher  $\gamma_0$ . This sensitive dependence can lead even to a network breakdown.

## 2.4 Role of $C \rightarrow B$ path

We have plotted  $\Delta$  in Fig.4(a) along with  $J_5$  in Fig.4(b) for different values of  $k_{-5}$  ( $> 0$ ). The relative positioning of the two points around which the sign changes of  $\Delta$  occur are given by Eq.(14) again. The BP zones are thus *finite*. It follows from Eq.(12) that, at large values of  $k_4$  (compared to the other rate constants),  $J_5$  becomes independent of  $k_4$  and then, using Eq.(13), one gets the limiting (positive) value of  $\Delta$  as

$$\Delta = \frac{\gamma_0 k_1 k_5}{k_2(k_1 + k_3)(k_2 + k_5)}. \quad (15)$$

## 2.5 Specific cases

In the rest of this section, we explore some specific cases. This will further improve our understanding of the variation of  $\Delta$  and the significance of the BP zone.

### 2.5.1 Case I: $k_5 = 0$ or $k_{-5} = 0$

This situation arises in an irreversible extra path. One finds here that  $J_5$  cannot change sign and remains either positive ( $k_{-5} = 0$ ) or negative ( $k_5 = 0$ ). Further,  $J_5$  becomes independent of  $k_4$  for  $k_{-5} = 0$  (see Fig.4(d)). So,  $\Delta$



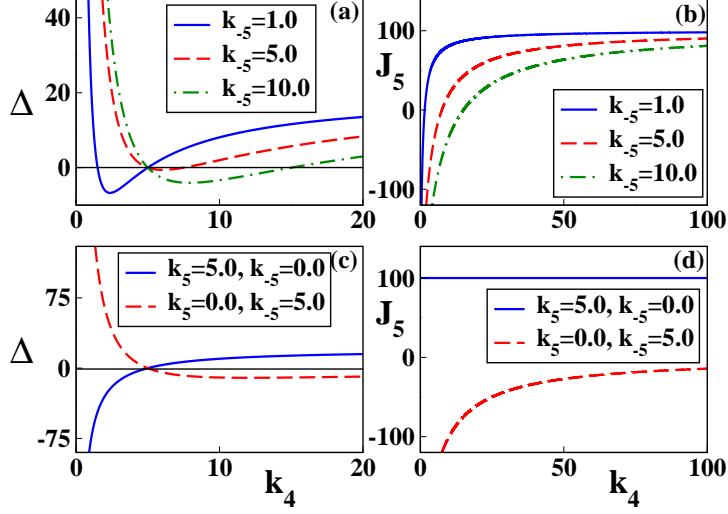


Figure 4: Variations of  $\Delta$  and  $J_5$  as a function of  $k_4$  in Scheme I. The values of the relevant parameters are as follows: (a), (b)  $k_1 = 1.0$ ,  $k_2 = 5.0$ ,  $k_3 = 1.5$ ,  $k_6 = 10.0$ ,  $k_5 = 5.0$ , all in  $\text{s}^{-1}$  and  $\gamma_0 = 500 \text{ Ms}^{-1}$ . (c), (d)  $k_1 = 1.0$ ,  $k_2 = 5.0$ ,  $k_3 = 1.5$ ,  $k_6 = 10.0$ , all in  $\text{s}^{-1}$  and  $\gamma_0 = 500 \text{ Ms}^{-1}$ .

changes sign only once at  $k_4 = k_2$ . For  $k_5 = 0$ ,  $\Delta$  is positive at low values of  $k_4$ , becomes zero at  $k_4 = k_2$  and then negative. This is shown in Fig.4(c). From Eq.(15), it follows that  $\Delta \rightarrow 0$  at large  $k_4$ . Hence, if  $k_4 \geq k_2$ ,  $\Delta \leq 0$  and the system supports an *infinite* BP zone. On the other hand, for  $k_{-5} = 0$ ,  $\Delta$  is negative at small  $k_4$  and  $\Delta = 0$  again at  $k_4 = k_2$  (see Fig.4(c)). So, the network remains in a *finite* BP zone for  $k_4 \leq k_2$ . Afterwards,  $\Delta$  becomes positive and attains the value given in Eq.(15) in the large- $k_4$  limit. Hence, the *nature of directionality* of the extra path strongly affects the emergence and sustenance of the BP zone. We mention that, when viewed as a function of  $k_2$ , the features simply get reversed. Also, for vanishing  $k_5$  or  $k_{-5}$ ,  $\Delta$  *cannot* change sign as a function of  $k_1$  or  $k_3$  (see Eq.(14)). When these parameters are varied, the system remains entirely either in the BP or in the non-BP zone, depending on the relative magnitudes of  $k_2$ ,  $k_4$ . For example, when  $k_5 = 0$ ,  $k_4 \geq k_2$ , the system remains *entirely* in the BP zone as a function of  $k_1$ . However, if  $k_4 < k_2$ , then the BP zone *vanishes completely*. These properties are shown in Fig.5(a). Similar plots are shown in Fig.5(b) for  $k_3$

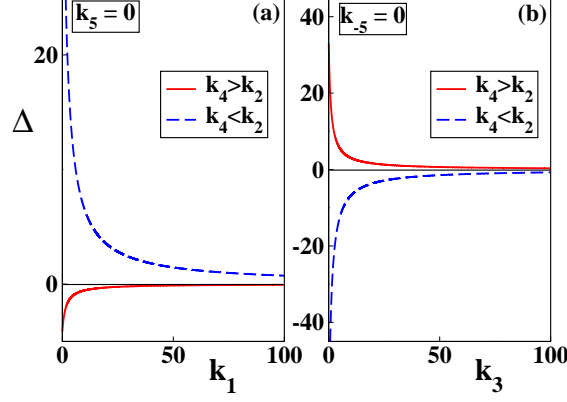


Figure 5: Variation of  $\Delta$  (a) as a function of  $k_1$  for  $k_5 = 0$  and (b) as a function of  $k_3$  for  $k_{-5} = 0$ . Depending on the relative magnitudes of  $k_2$  and  $k_4$ , the system can be entirely in the BP or in the non-BP zone. The values of the relevant parameters are as follows: (a)  $k_2 = 5.0$ ,  $k_3 = 1.5$ ,  $k_6 = 10.0$ ,  $k_{-5} = 1.0$ ,  $k_4 = 2.0$  and,  $15.0$ , all in  $\text{s}^{-1}$ ; (b)  $k_1 = 1.0$ ,  $k_2 = 5.0$ ,  $k_6 = 10.0$ ,  $k_5 = 5.0$ ,  $k_4 = 2.0$  and,  $15.0$ , all in  $\text{s}^{-1}$ .  $\gamma_0 = 500 \text{ Ms}^{-1}$  in both the cases.

at  $k_{-5} = 0$ . For further details, we refer the reader to Table 1.

### 2.5.2 Case II: $k_1 k_5 = k_3 k_{-5}$

In this special case, the two points given in Eq.(14) merge to a single point,  $k_4 = k_2$ . Using Eq.(12) and Eq.(13) along with the above condition, we get

$$\Delta = \frac{\gamma_0 (k_4 - k_2)^2 k_1 k_5}{k_2 k_4 (k_1 + k_3) (k_2 (k_4 + k_{-5}) + k_4 k_5)}. \quad (16)$$

Hence, in this situation,  $\Delta$  *cannot* be negative. The presence of the extra path decreases the load for all values of  $k_4$  except at  $k_4 = k_2$  where  $\Delta = 0$  and the BP zone reduces to a point. These features are shown in Fig.6 for specific values of the relevant parameters:  $k_1 = 1.0$ ,  $k_2 = 5.0$ ,  $k_3 = 2.5$ ,  $k_6 = 10.0$ ,  $k_5 = 5.0$ ,  $k_{-5} = 2.0$ , all in  $\text{s}^{-1}$  and  $\gamma_0 = 500 \text{ Ms}^{-1}$ .

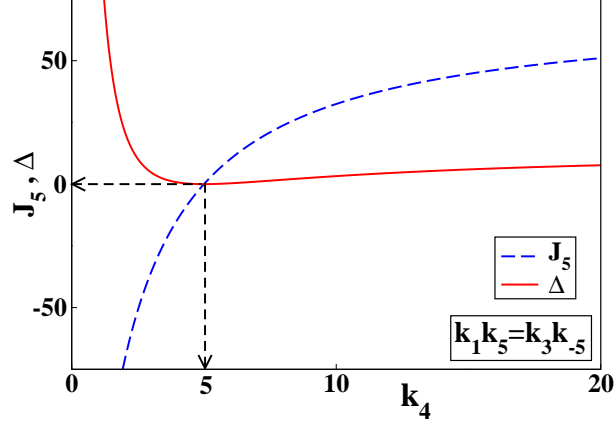


Figure 6: Variations of  $\Delta$  and  $J_5$  as a function of  $k_4$  in Scheme I for the case  $k_1k_5 = k_3k_{-5}$ . The values of the relevant parameters are as follows:  $k_1 = 1.0$ ,  $k_2 = 5.0$ ,  $k_3 = 2.5$ ,  $k_6 = 10.0$ ,  $k_5 = 5.0$ ,  $k_{-5} = 2.0$ , all in  $\text{s}^{-1}$  and  $\gamma_0 = 500 \text{ Ms}^{-1}$ .

### 2.5.3 Case III: $k_1 = k_4$ , $k_3 = k_2$

This diagonally symmetric case resembles the networks commonly used to show the occurrence of BP [43]. Here, the points where  $\Delta$  is zero are given by

$$k_4 = k_2 \left( \frac{k_{-5}}{k_5} \right)^{1/2} \quad \text{and} \quad k_4 = k_2. \quad (17)$$

Hence,  $\Delta$  changes sign twice as a function of  $k_4$ . If either  $k_5$  or  $k_{-5}$  vanishes, then  $\Delta$  can change sign once (at  $k_4 = k_2$ ). The two points in Eq.(17) merge at  $k_5 = k_{-5}$  whence  $\Delta \geq 0$ . So, the main results remain unchanged in this symmetric case. A summary of all our findings on Scheme I can be found in Table 1.

## 3 Selective introduction of reversibility

The CRN, denoted as Scheme II, is shown in Fig.7. This type of symmetric CRN was used recently in the same context [43] where the reversible steps

Table 1: Summary of the results in the various cases of Scheme I regarding the appearance of BP zone as a function of different system parameters and the dependence on the nature of extra path. Here,  $f = k_3 k_{-5} / (k_1 k_5)$ ,  $k_4^* = f k_2$ ,  $k_4^{**} = k_2$ ,  $k_2^* = k_4 / f$ ,  $k_2^{**} = k_4$ ,  $k_1^* = k_2 k_3 k_{-5} / (k_4 k_5)$ ,  $k_3^* = k_1 k_4 k_5 / (k_2 k_{-5})$ .

Network parameter	Nature of extra path	BP zone condition
$k_4$	$k_{\pm 5} > 0$	$k_4^* \leq k_4 \leq k_4^{**} \ (f < 1)$ $k_4^{**} \leq k_4 \leq k_4^* \ (f > 1)$
	$k_5 = 0$	$k_4 \geq k_4^{**}$
	$k_{-5} = 0$	$k_4 \leq k_4^{**}$
	$k_5 / k_{-5} = k_3 / k_1$	$k_4 = k_4^{**}$
$k_2$	$k_{\pm 5} > 0$	$k_2^* \leq k_2 \leq k_2^{**} \ (f > 1)$ $k_2^{**} \leq k_2 \leq k_2^* \ (f < 1)$
	$k_5 = 0$	$k_2 \leq k_2^{**}$
	$k_{-5} = 0$	$k_2 \geq k_2^{**}$
	$k_5 / k_{-5} = k_3 / k_1$	$k_2 = k_2^{**}$
$k_1$	$k_{\pm 5} > 0$	$k_1 \leq k_1^* \ (k_4 \geq k_2)$ $k_1 \geq k_1^* \ (k_4 \leq k_2)$
	$k_5 = 0$	$k_4 \geq k_2$
	$k_{-5} = 0$	$k_4 \leq k_2$
$k_3$	$k_{\pm 5} > 0$	$k_3 \geq k_3^* \ (k_4 > k_2)$ $k_3 \leq k_3^* \ (k_4 < k_2)$
	$k_5 = 0$	$k_4 \geq k_2$
	$k_{-5} = 0$	$k_4 \leq k_2$

are taken to mimic traffic congestion. Due to the reversible steps, the fluxes  $J_1(t)$  and  $J_4(t)$  get modified as

$$J_1(t) = k_1 a(t) - k_{-1} b(t); \quad J_4(t) = k_1 c(t) - k_{-1} e(t). \quad (18)$$

The other fluxes remain the same as in Scheme I, but with  $k_2 = k_3$ . At SS, again we get  $J_0 = J_6$ . The SS concentrations in this case are given by

$$b = \frac{\gamma_0 k_1^2 + (k_1 + k_3)(k_{-1} + k_6)k_{-5}e}{k_1^2(k_3 + k_5) + k_1 k_3(k_{-1} + k_3 + k_5) + (k_1 + k_3)k_3 k_{-5}}, \quad (19)$$

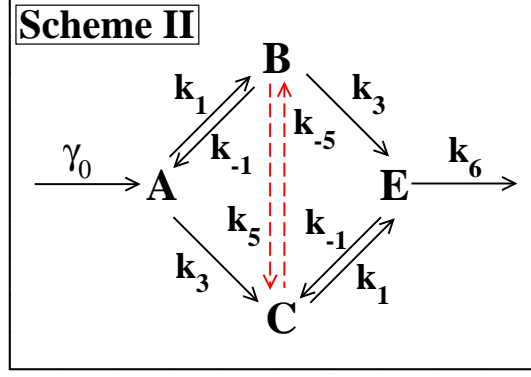


Figure 7: Schematic diagram of the symmetric CRN with some reversible steps. The extra path is shown by the dashed, red line.

$$a = \frac{\gamma_0 + k_{-1}b}{k_1 + k_3}; \quad k_1c = (k_{-1} + k_6)e - k_3b \quad (20)$$

where  $e$  is given by Eq.(10). From Eq.(19), one gets

$$b^0 = \frac{\gamma_0 k_1}{k_3(k_1 + k_{-1} + k_3)}. \quad (21)$$

### 3.1 Relation between load-difference and extra path flux

At SS, the flux  $J_5$  can be written as

$$\begin{aligned} J_5 &= J_4 - J_3 = J_6 - J_2 - J_3 \\ &= \gamma_0 - k_3(a + b) \\ &= \frac{\gamma_0 k_1}{k_1 + k_3} \left( 1 - \frac{b}{b^0} \right) \end{aligned} \quad (22)$$

where the last line is obtained by using Eqs.(20)-(21). The load-difference  $\Delta$  turns out here as

$$\Delta = \left( \frac{k_1(k_1 + k_{-1}) - k_3^2}{k_1(k_1 + k_3)} \right) (b^0 - b)$$

$$= \left( \frac{k_1(k_1 + k_{-1}) - k_3^2}{\gamma_0 k_1^2} \right) b^0 J_5. \quad (23)$$

### 3.2 Exploring BP zones

We now calculate the points in the parameter space where  $\Delta = 0$  to find the BP zone(s). Putting Eq.(19) and Eq.(21) into Eq.(23) and setting the latter equal to zero, we get the equation

$$(k_1(k_1 + k_{-1}) - k_3^2)X = 0. \quad (24)$$

Here

$$X = P_1 k_3^2 + Q_1 k_3 + R_1 \quad (25)$$

with

$$P_1 = \gamma_0 k_{-5}; Q_1 = k_{-5} k_{-1} e(k_1 + k_{-1} + k_3 + k_6); R_1 = -\gamma_0 k_5 k_1^2. \quad (26)$$

If the variation of  $\Delta$  is studied as a function of  $k_3$ , then from Eqs.(24)-(25), we get the two points where  $\Delta$  becomes zero as

$$k_3 = (k_1(k_1 + k_{-1}))^{1/2}; k_3 = \frac{-Q_1 + (Q_1^2 - 4P_1 R_1)^{1/2}}{2P_1}. \quad (27)$$

Therefore,  $\Delta$  changes sign twice with  $k_3$ . At the second value of  $k_3$  in Eq.(27),  $J_5 = 0$ . We have plotted  $\Delta$  and  $J_5$  with  $k_3$  in Fig.8.

One can also get similar behavior as a function of other rate constants. For example, it follows from Eqs.(24)-(25) that  $\Delta$  is zero at the following pair of values of  $k_1$

$$k_1 = \frac{-k_{-1} + (k_{-1}^2 + 4k_3^2)^{1/2}}{2}; k_1 = \frac{-Q_2 - (Q_2^2 - 4P_2 R_2)^{1/2}}{2P_2}, \quad (28)$$

where

$$P_2 = -\gamma_0 k_5; Q_2 = k_{-1} k_3 k_{-5} e; R_2 = k_3 k_{-5} (k_{-1}^2 e + \gamma_0 k_3 + k_{-1} k_3 e + k_{-1} \gamma_0). \quad (29)$$

Similarly, one obtains the equivalent points in terms of  $k_{-1}$  as

$$k_{-1} = \frac{k_3^2 - k_1^2}{k_1}; k_{-1} = \frac{-Q_3 + (Q_3^2 - 4P_3 R_3)^{1/2}}{2P_3}, \quad (30)$$

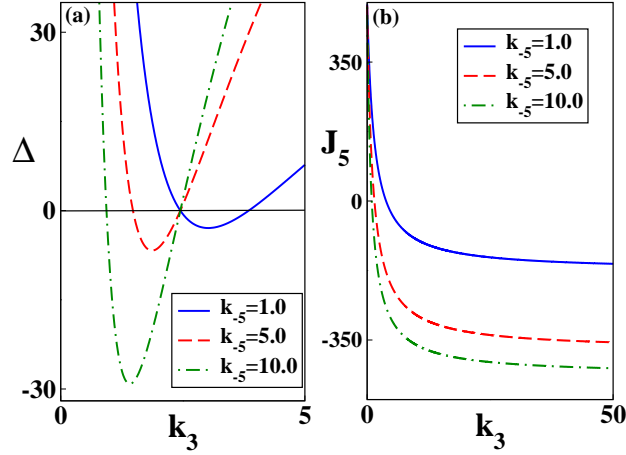


Figure 8: Variations of  $\Delta$  and  $J_5$  as a function of  $k_3$  in Scheme II. The values of the relevant parameters are as follows:  $k_1 = 2.0$ ,  $k_{-1} = 5.0$ ,  $k_6 = 20.0$ ,  $k_5 = 5.0$ , all in  $\text{s}^{-1}$  and  $\gamma_0 = 500 \text{ Ms}^{-1}$ .

where

$$P_3 = k_3 k_{-5} e; Q_3 = k_3 k_{-5} (k_1 e + k_3 e + \gamma_0); R_3 = \gamma_0 (k_{-5} k_3^2 - k_5 k_1^2). \quad (31)$$

However, this last equation shows that, for  $\Delta$  to change sign twice, one needs  $R_3 < 0$  for a physically meaningful value of  $k_{-1}$ . It is easy to see that, for an irreversible extra path (vanishing  $k_5$  or  $k_{-5}$ ),  $\Delta$  can change sign only once with the variation of any of the three parameters. The  $\Delta = 0$  points are given by the first values in Eq.(27), Eq.(28) and Eq.(30), in the respective cases.

## 4 Introduction of extra nodes

It is appropriate now to ask: how the basic features of the SS load will be affected in presence of additional nodes (species)? In this section, we try to answer this question. To do so, we consider an extended, six-node version of the CRN in Scheme I, denoted as Scheme III. The schematic is depicted in Fig.9. To maintain the connection with the previous schemes, the route with rate constants  $k_{\pm 7}$  is taken as the extra path. This enables one

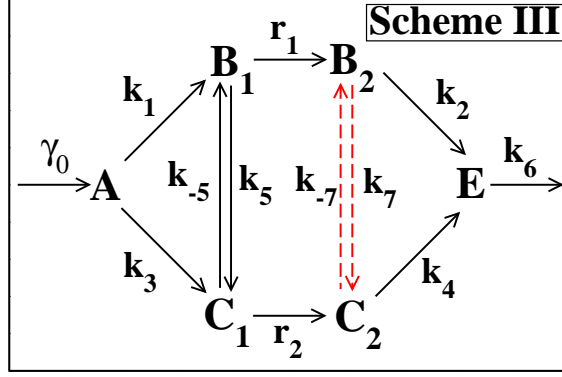


Figure 9: Schematic diagram of the extended, six-node CRN. The extra path is shown by the dashed, red line.

to understand the role of the network structure in governing the SS load  $Z$ , particularly by comparing the results of this scheme with Scheme I. Following similar procedures as before, one obtains the SS concentrations as

$$a = \gamma_0 / (k_1 + k_3), \quad e = \gamma_0 / k_6, \quad (32)$$

$$c_1 = \frac{\gamma_0 k_5 + r_1 k_3 a}{r_1(r_2 + k_{-5}) + r_2 k_5}, \quad b_1 = \frac{k_1 a + k_{-5} c_1}{r_1 + k_5}, \quad (33)$$

$$c_2 = (\gamma_0 k_7 + k_2 r_2 c_1) / Y, \quad b_2 = (\gamma_0 - k_4 c_2) / k_2 \quad (34)$$

where

$$Y = k_2(k_4 + k_{-7}) + k_4 k_7. \quad (35)$$

Let us remind the reader that the variables at  $k_{\pm 7} = 0$  are denoted by a zero superscript with  $a^0 = a$ ,  $e^0 = e$ ,  $c_1^0 = c_1$ ,  $b_1^0 = b_1$  (see Eqs.(32)-(34)). From Eqs.(32)-(35), the effect of the extra path on  $Z$  is determined by the following load-difference

$$\begin{aligned} \Delta &= Z^0 - Z = (b_1^0 + c_1^0 + b_2^0 + c_2^0) - (b_1 + c_1 + b_2 + c_2) \\ &= \left( \frac{k_4 - k_2}{Y k_2} \right) \left( \gamma_0 k_7 - \frac{r_2(k_4 k_7 + k_2 k_{-7})}{k_4} c_1 \right). \end{aligned} \quad (36)$$



It follows from Eq.(36) that  $\Delta$  becomes zero at  $k_4 = k_2$  and also when

$$c_1 = \frac{\gamma_0 k_4 k_7}{r_2(k_4 k_7 + k_2 k_{-7})}. \quad (37)$$

Equating the two expressions of  $c_1$  in Eq.(37) and Eq.(33), we obtain the required condition as

$$r_1 k_4 k_7 (k_1 r_2 + k_1 k_{-5} + k_3 k_{-5}) = r_2 k_2 k_{-7} (r_1 k_3 + k_1 k_5 + k_3 k_5). \quad (38)$$

So, as a function of  $k_4$  or  $k_2$ , we again find that  $\Delta$  can change sign twice. Also, for either  $k_7 = 0$  or  $k_{-7} = 0$ ,  $\Delta$  can change sign only once (see Eq.(38)). Thus, the qualitative behavior of  $\Delta$  *remains the same* as that obtained via Scheme I or Scheme II.

## 5 A biochemical application: Uric acid degradation in purine catabolism

The purine catabolism in many organisms involves the stereospecific breakdown of uric acid to produce allantoin as the key step [48]. Notable exceptions are humans, birds, reptiles and some bacteria. This is the reason why accumulation of urate can lead to gout and renal stones in humans. The reaction pathway for oxidative decomposition of urate is shown schematically in Fig.10. This is based on the recent work by Bovigny *et al.* [49]. The species consisting the CRN, denoted as Scheme IV, in Fig.10 are:  $A_0$  : Uric acid, A: 5-hydroxyisourate (HIU), B: 2-oxo-4-hydroxy-4-carboxy-5-ureidoimidazoline (OHCU), C: (*R*)-Allantoin, E: (*S*)-Allantoin,  $E_0$  : Allantoate. The enzymatic conversion of allantoin to allantoate ( $E_0$ ) is stereospecific for the (*S*)-isomer (E). However, both the (*S*)- and the (*R*)-isomer are produced from the spontaneous (non-enzymatic) decomposition of HIU (A) and OHCU (B) and also via racemization. The details of the reaction steps and catalysts involved are given in Table 2.

In our context, the decomposition steps  $A \rightarrow E$  and  $B \rightarrow C$  constitute the extra paths (shown by dashed, red lines in Fig.10). These paths result in the *indiscriminate* formation of species C and E from B and A, respectively. As the enzymatic degradations are stereospecific, the decomposition steps appear to be disadvantageous. Next, we will try to understand whether these pathways can have some *functional* role, *i.e.*, the system can use them

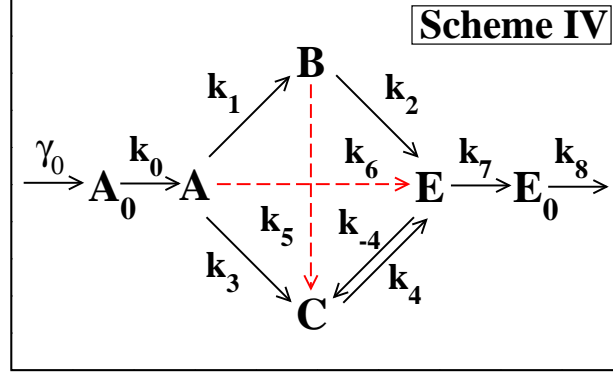


Figure 10: Schematic diagram of the uric acid degradation pathway, highly important in purine catabolism, based on Ref.[49]. The species involved are:  $A_0$  : Uric acid, A: HIU, B: OHCU, C: (*R*)-Allantoin, E: (*S*)-Allantoin,  $E_0$  : Allantoate. The extra paths (dashed, red lines) represent the spontaneous decomposition of intermediates A and B.

for some kind of advantage. In what follows, the concentrations of different enzymes (and other species) involved in various steps of the network are taken as constants (acting as chemiostats) and included in the pseudo-first-order rate constants  $k_i$ . The variations of  $k_i$  are thus naturally linked to the corresponding *parametric* variations in enzyme concentration.

## 5.1 Decomposition paths and BP zone

The SS concentrations are determined following similar procedures as earlier. They are given by

$$\begin{aligned}
 a_0 &= \frac{\gamma_0}{k_0}, \quad e = \frac{\gamma_0}{k_7}, \quad e_0 = \frac{\gamma_0}{k_8}, \\
 a &= \frac{\gamma_0}{k_1 + k_3 + k_6}, \quad b = \frac{k_1 a}{k_2 + k_5}, \\
 c &= \frac{k_3 a + k_5 b + k_{-4} e}{k_4}.
 \end{aligned} \tag{39}$$

Table 2: Details of the CRN in Scheme IV representing uric acid degradation, based on Ref.[49]. The abbreviations ‘sp’ and ‘en’ mean ‘spontaneous’ and ‘enzymatic’, respectively. The actual rate constants of enzymatic steps are denoted as  $k'_i$  and those of the spontaneous decomposition steps as  $k_i^0$ .

Reaction	Nature	Catalyst	Effective rate constant
$A_0 \rightarrow A$	hydroxylation	Uricase ( $E_1$ )	$k_0 = k'_0[E_1]$
$A \rightarrow B$	hydrolysis	HIU hydrolase ( $E_2$ )	$k_1 = k'_1[E_2]$
$A \rightarrow C$	decomposition (sp)	—	$k_3 = k_3^0$
$B \rightarrow C$	decomposition (sp)	—	$k_5 = k_5^0$
$B \rightarrow E$	decarboxylation + decomposition (sp)	OHCU decarboxylase ( $E_3$ )	$k_2 = k_2^0 + k'_2[E_3]$
$A \rightarrow E$	decomposition (sp)	—	$k_6 = k_6^0$
$C \rightarrow E$	racemization (en)+ racemization (sp)	Allantoin racemase ( $E_4$ )	$k_4 = k_4^0 + k'_4[E_4]$
$E \rightarrow E_0$	hydrolysis	Allantoinase ( $E_5$ )	$k_7 = k'_7[E_5]$

Using Eq.(39), the effect of the extra paths is determined by  $\Delta$  as

$$\begin{aligned}
\Delta &= Z(k_5 = k_6 = 0) - Z = Z^0 - Z \\
&= (a^0 + b^0 + c^0) - (a + b + c) \\
&= \frac{\gamma_0(s_1 k_2^2 + s_2 k_2 + s_3)}{k_2 k_4 (k_1 + k_3)(k_2 + k_5) s_4}
\end{aligned} \tag{40}$$

with the symbols having the same meanings as before. Here

$$\begin{aligned}
s_1 &= k_6(k_3 + k_4), \quad s_2 = k_5(k_4 k_6 + k_3 k_6 - k_1^2 - k_1 k_3) + k_1 k_4 k_6, \\
s_3 &= k_1 k_4 k_5 s_4, \quad s_4 = (k_1 + k_3 + k_6).
\end{aligned} \tag{41}$$

Now, we investigate the possibility of BP zones in this network. As  $s_1, s_3 > 0$ , it follows from Eqs.(40)-(41) that,  $\Delta$  can't be zero for  $s_2 \geq 0$  when viewed as a function of  $k_2$ . Actually, here  $\Delta$  remains positive and there is *no scope* for BP zone to develop. Equation (41) suggests that this will occur for sufficiently large  $k_5, k_6$  values compared to the other rate constants.

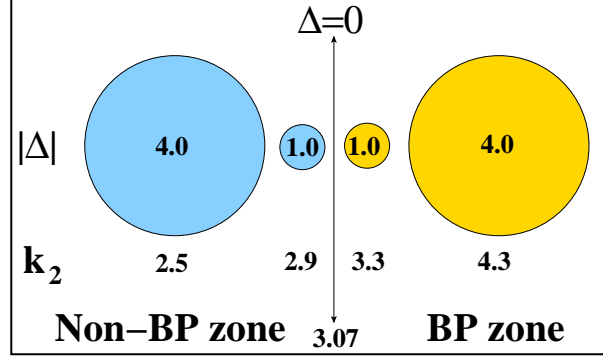


Figure 11: The variation in the magnitude of  $\Delta$  as a function of  $k_2$ ;  $|\Delta|$  is proportional to the radii of the circles (written inside). The  $\Delta = 0$  points appear at  $k_2 = 3.07 \text{ s}^{-1}$ , shown in the figure, and at  $k_2 = 1085.43 \text{ s}^{-1}$ , for the set of parameters as follows:  $k_1 = 10.0$ ,  $k_3 = 1.0$ ,  $k_4 = 3.0$ ,  $k_{-4} = 2.0$ ,  $k_5 = 4.0$ ,  $k_6 = 0.1$ ,  $k_7 = 1.5$ , all in  $\text{s}^{-1}$  and  $\gamma_0 = 100 \text{ Ms}^{-1}$ .

Hence, the *indiscriminate decomposition pathways can play a functional role in reducing the SS load of the network*. If  $s_2 < 0$ , then it is possible for  $\Delta$  to change sign twice with the variation of  $k_2$  and *finite* BP zones appear. See Fig.11. The numerator in Eq.(40) is also quadratic in  $k_1$ . It can be easily checked that, depending on the relative magnitudes of  $k_2$  and  $k_4$ ,  $\Delta$  can change sign once or twice with  $k_1$ . In this case, *infinite* BP zones can also emerge. Therefore, the variation in concentrations of different enzymes affects the system load in a distinct manner.

As there are two extra paths, another interesting feature is the effect of one in presence of the other. Let us first take the extra path BC. One obtains the effect of the BC path in presence of the AE path ( $k_6 > 0$ ) as

$$\Delta_1 = Z(k_5 = 0) - Z = \frac{(k_4 - k_2)k_1k_5a}{k_2k_4(k_2 + k_5)}. \quad (42)$$

$\Delta_1$  becomes zero at  $k_4 = k_2$  and changes sign once against  $k_2$  or  $k_4$ . *Infinite* BP zone appears when viewed as a function of  $k_2$  whereas, the system supports a *finite* BP zone as a function of  $k_4$ .

Next, we study the effect of the AE path in presence of the BC path ( $k_5 > 0$ ). In this case, the load-difference becomes

$$\Delta_2 = Z(k_6 = 0) - Z$$

$$= \left( \frac{\gamma_0 k_6}{s_4(k_1 + k_3)} \right) \left[ \left( 1 + \frac{k_3}{k_4} \right) + \left( 1 + \frac{k_5}{k_4} \right) \left( \frac{k_1}{k_2 + k_5} \right) \right] > 0. \quad (43)$$

Thus, in presence of the BC path, addition of the path AE *always* reduces the SS load and *no* BP zone exists. The above-mentioned features indicate that the SS load can play a major role, along with other factors, in governing the evolution of optimized reaction steps in living systems.

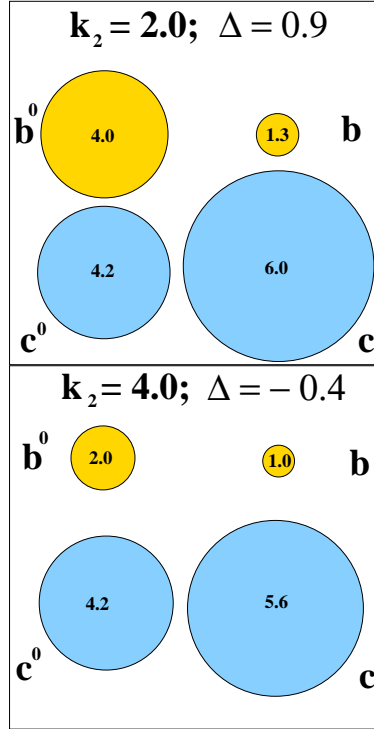


Figure 12: The SS concentrations of species B, C in absence and in presence of the extra paths (see Fig.10). The concentrations are proportional to the radii of the corresponding circles (written inside). In the top panel, the system is in the non-BP zone whereas, in the bottom panel, it is in the BP zone. The values of the relevant parameters are as follows:  $k_1 = 10.0$ ,  $k_3 = 1.0$ ,  $k_4 = 3.0$ ,  $k_{-4} = 2.0$ ,  $k_5 = 4.0$ ,  $k_6 = 0.1$ ,  $k_7 = 1.5$ , all in  $s^{-1}$  and  $\gamma_0 = 100 \text{ Ms}^{-1}$ . The SS concentration of species A alters little and hence not shown.

## 5.2 The load distribution

Here, we make a brief survey on the distribution of the load over the CRN, *i.e.*, on the individual SS concentrations. According to Eq.(39), only  $a$ ,  $b$ ,  $c$  depend on the parameters of the extra paths. In absence the extra paths ( $k_5 = k_6 = 0$ ),  $a$ ,  $b$  increase whereas  $c$  decreases. However, their *relative change in magnitudes* dictate the fate of  $\Delta$ . In Fig.12, the changes in the SS concentrations due to the addition of the extra paths are shown at two values of  $k_2$ . For the parameters chosen, particularly at the small  $k_6$  value,  $a \approx a^0$  and hence not shown in the figure. Both in the top and bottom panels of Fig.12, we have  $b^0 > b$ ,  $c^0 < c$ . But, the system is in the BP zone only in the bottom panel. This shows that, focusing on a single species concentration can be misleading in detecting the BP zone.

## 5.3 The load dynamics

Before concluding, we touch upon the dynamics of the load. The individual time-evolutions of the reacting species of Scheme IV are determined numerically. The load  $Z(t)$  is plotted in Fig.13 as a function of time for three different cases:  $\Delta > 0$ ,  $\Delta = 0$ ,  $\Delta < 0$ . The set of parameters are the same as in the previous two subsections. In all the cases,  $\Delta$  shows a monotonic rise till the system reaches the SS. When the system is in the non-BP zone (Fig.13a),  $Z$  remains lower throughout if extra paths are present. Similarly, in the BP zone (Fig.13c),  $Z$  is greater in presence of extra paths during the whole reaction progression. Interestingly, for  $\Delta = 0$  (Fig.13b),  $Z$  follows virtually the same time-course with and without the extra paths. Thus, regarding the BP zones, the load dynamics in our case is in conformity with the results obtained so far and does not provide any qualitatively new information. However, for brevity, we refrain from a detailed analysis of the load dynamics as a function of various system parameters.

## 6 Discussion and Conclusion

In this study, we have investigated the effect of additional paths on the SS load of open CRNs. The problem is related to the handling of traffic flow in general and particularly the paradoxical case illustrated by Braess, where inclusion of extra routes increases the travel time. In an equivalent manner, we have found BP-like behavior in the SS load which, instead of dropping,

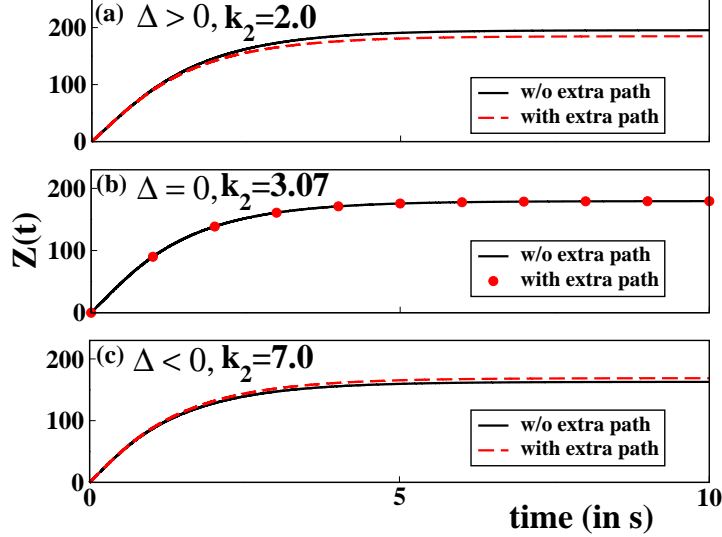


Figure 13: Time-evolution of  $Z(t)$  in absence and in presence of the extra paths (see Fig.10). The three cases are: (a)  $\Delta > 0$ ,  $k_2 = 2.0 \text{ s}^{-1}$ , (b)  $\Delta = 0$ ,  $k_2 = 3.07 \text{ s}^{-1}$ , (c)  $\Delta < 0$ ,  $k_2 = 7.0 \text{ s}^{-1}$ . The values of the other parameters are as follows:  $k_0 = 15.0$ ,  $k_1 = 10.0$ ,  $k_3 = 1.0$ ,  $k_4 = 3.0$ ,  $k_{-4} = 2.0$ ,  $k_5 = 4.0$ ,  $k_6 = 0.1$ ,  $k_7 = 1.5$ ,  $k_8 = 5.0$ , all in  $\text{s}^{-1}$  and  $\gamma_0 = 100 \text{ Ms}^{-1}$ .

can get raised or remains the same due to the presence of extra paths. The region of parameter space where this kind of behavior occurs is denoted as the BP zone. Taking some basic networks, we have explored the roles of the system parameters in governing the materialization of such zones. First of all, the load difference  $\Delta$  is found to be proportional to the rate of influx  $\gamma_0$ . Thus, the BP-zone (as well as the non-BP zone) grows with  $\gamma_0$ . Investigating the effects of the paths forming network-edges, we have found an appealing aspect regarding the variation of the associated rate constants. For some of them ( $k_2$ ,  $k_4$  in Scheme I), the BP zone is *finite* as  $\Delta$  changes sign twice. It can even reduce to a point. For the others ( $k_1$ ,  $k_3$  in Scheme I),  $\Delta$  can change sign *only* once and then the BP zone can turn *infinite*. Making some steps reversible and symmetric (as in Scheme II) generates *finite* BP zones as a function of all the rate constants of the network edges. However, for an irreversible extra path,  $\Delta$  can change sign only once in both the schemes. Then *finite* BP zones become *infinite* again. The basic features are shown to

remain unchanged in an extended six-node version of the network (Scheme III).

The nature of the extra path is of immense importance regarding the existence of the BP zone. This is manifested in the intimate connection between  $\Delta$  and  $J_5$ , the flux associated with the extra path (see Eq.(13) and Eq.(23)). For a reversible extra path, the BP zone *cannot* span the entire parameter ( $k_i$ ) range although it can stretch infinitely. This is not always the case with an irreversible extra path. Depending on the direction of the extra path, the system can show two extreme behaviors. (i) It is *always* in the BP zone over the whole range of some parameter; (ii) It does *not* support any BP zone over the whole range of the same parameter. Between (i) and (ii), the kind of behavior actually shown by the system depends on the relative values of other parameters (case of  $k_1$ ,  $k_3$  in Scheme I, see Table 1). This kind of ‘switching’ response of the system to the addition of extra path is highly interesting as well as of huge practical impact in the designing and planning of network geometries. We have also applied the methodology on the important biochemical network of uric acid degradation. From the detailed analyses of the corresponding CRN in an open system framework, we propose that some of the spontaneous decomposition steps of the intermediates can have *functional roles* in reducing the SS load. As the magnitude of the SS load is essential for the physical sustainability of the reaction medium, this can be one of the major deciding factors in the evolution of various reaction mechanisms in living systems.

## Acknowledgment

K. Banerjee acknowledges the University Grants Commission (UGC), India for Dr. D. S. Kothari Fellowship. K. Bhattacharyya thanks CRNN, CU, for partial financial support.

## References

- [1] L. von Bertalanffy, Science **111**, 23 (1950).
- [2] F. J. M. Horn and R. Jackson, Arch. Ration. Mech. Anal. **47**, 81 (1972).
- [3] M. Feinberg and F. J. M. Horn, Chem. Eng. Sci. **29**, 775 (1974).



- [4] B. L. Clarke, Adv. Chem. Phys. **43**, 1 (1980).
- [5] S. Schuster and R. Schuster, J. Math. Chem. **6**, 17 (1991).
- [6] U. S. Bhalla, Prog. Biophys. Mol. Biol. **81**, 45 (2003).
- [7] G. P. Wagner, M. Pavlicev, and J. M. Cheverud, Nature Rev. Genetics **8**, 921 (2007).
- [8] A. Goldbeter, *Biochemical Oscillations and Cellular Rhythms. The Molecular Bases of Periodic and Chaotic Behavior*, (Cambridge Univ. Press, Cambridge, UK, 1996).
- [9] B. Edelstein, J. Theor. Biol. **29**, 5762 (1970).
- [10] M. Feinberg, Chem. Eng. Sci. **42** 2229 (1987).
- [11] M. Merrow and M. Brunner, FEBS Lett. **585**, 1383 (2011).
- [12] L. M. Kellershohn, Trends Biochem. Sci. **24**, 418 (1999).
- [13] H. Jeong, B. Tombor, R. Albert, Z. N. Oltvai, and A.-L. Barabasi, Nature **407**, 651 (2000).
- [14] E. Brown, R. Kass, and P. Mitra, Nature Neurosci. **7**, 456 (2004).
- [15] P. Francois and V. Hakim, Proc. Natl Acad. Sci. (USA) **101**, 580 (2004).
- [16] A. Slusarczyk, A. Lin, and R. Weiss, Nature Rev. Genet. **13**, 406 (2012).
- [17] D. Meyer, P. Neumann, E. Koers, H. Sjuts, S. Ludtke, G. M. Sheldrick, R. Ficner, and K. Tittmann, Proc. Natl. Acad. Sci. U.S.A. **109**, 10867 (2012).
- [18] D. Jacquemin, J. Zuniga, A. Requena, and J. P. Ceron-Carrasco, Acc. Chem. Res. (2014) DOI: 10.1021/ar500148c.
- [19] A. Katchalsky and Peter F. Curran, *Non-equilibrium thermodynamics in Biophysics*, (Harvard University Press, Cambridge, MA, 1965.)
- [20] G. Nicolis and I. Prigogine, *Self-organization in Non-equilibrium Systems (from Dissipative Structures to order through Fluctuations)*, (John Wiley and Sons, New York, 1977.)

- [21] C. Y. Mou, J. -L. Luo, and G. Nicolis, *J. Chem. Phys.* **84**, 7011 (1986).
- [22] J. Ross and M. O. Vlad, *Ann. Rev. Phys. Chem.* **50**, 51 (1999).
- [23] P. Gaspard, *J. Chem. Phys.* **120**, 8898 (2004).
- [24] D. Andrieux and P. Gaspard, *J. Chem. Phys.* **121**, 6167 (2004).
- [25] T. Schmiedl, and U. Seifert, *J. Chem. Phys.* **126**, 044101 (2007).
- [26] D. Andrieux and P. Gaspard, *J. Chem. Phys.* **130**, 014901 (2009).
- [27] H. Qian, *Annu. Rev. Phys. Chem.* **58**, 113 (2007).
- [28] M. Vellela and H. Qian, *J. R. Soc. Interface* **6**, 925 (2009).
- [29] J. J. Hopfield, *Proc. Natl. Acad. Sci. U.S.A.* **71**, 4135 (1974).
- [30] T. Hill, *Proc. Natl. Acad. Sci. U.S.A* **80**, 2922 (1983).
- [31] L. Jullien, A. Lemarchand, S. Charier, O. Ruel, and J.-B. Baudin, *J. Phys. Chem. B* **107**, 9905 (2003).
- [32] D. Andrieux and P. Gaspard, *Proc. Natl. Acad. Sci. U.S.A.* **105**, 9516 (2008).
- [33] H. Qian and E. L. Elson, *Biophys. Chem.* **101**, 565 (2002).
- [34] W. Min, L. Jiang, J. Yu, S. C. Kou, H. Qian, and X. S. Xie, *Nano Lett.* **5**, 2373 (2005).
- [35] K. Banerjee, B. Das, and G. Gangopadhyay, *J. Chem. Phys.* **136**, 154502 (2012).
- [36] M. Polettini and M. Esposito, *J. Chem. Phys.* **141**, 024117 (2014).
- [37] M. Timme and J. Casadiego, *J. Phys. A: Math. Theor.* **47**, 343001 (2014).
- [38] D. Braess, *Unternehmensforschung* **12**, 258 (1968); English translation in: D. Braess, A. Nagurney, and T. Wakolbinger, *Transportation Sci.* **39**, 446 (2005).
- [39] T. Roughgarden, *J. Comput. System Sci.* **72**, 922 (2006).

- [40] C. M. Penchina and L. J. Penchina, Am. J. Phys. **71**, 479 (2003).
- [41] D. Witthaut and M. Timme, New J. Phys. **14**, 083036 (2012).
- [42] M. G. Pala, S. Baltazar, P. Liu, H. Sellier, B. Hackens, F. Martins, V. Bayot, X. Wallart, L. Desplanque, and S. Huant, Phys. Rev. Lett. **108**, 076802 (2012).
- [43] D. M. Lepore, C. Barratt, and P. M. Schwartz, J. Math. Chem. **49**, 356 (2011).
- [44] R. F. Martinez, M. Avalos, R. Babiano, P. Cintas, M. E. Light, J. L. Jimenez, and J. C. Palacios, Tetrahedron **70**, 2319 (2014).
- [45] R. A. Jones and A. Whitmore, ARKIVOC **11**, 114 (2007); DOI: <http://dx.doi.org/10.3998/ark.5550190.0008.b10>
- [46] A. R. E. Carey, S. Eustace, R. A. M. O’Ferrall, and B. A. Murray, J. Chem. Soc. Perkin Trans. **2**, 2285 (1993) .
- [47] N. Nemeria, E. Binshtein, H. Patel, A. Balakrishnan, I. Vered, B. Shaanan, Z. Barak, D. Chipman, and F. Jordan, Biochemistry **51**, 7940 (2012).
- [48] P. A. Tipton, Nat. Chem. Biol. **2**, 124 (2006).
- [49] C. Bovigny, M. T. Degiacomi, T. Lemmin, M. Dal Peraro, and M. Stenta, J. Phys. Chem. B **118**, 7457 (2014).